Density functional theory study of NO_2-sensing mechanisms of pure and Ti-doped WO_3 (002) surfaces*

Hu Ming(胡 明)†, Wang Wei-Dan(王巍丹), Zeng Jing(曾 晶), and Qin Yu-Xiang(秦玉香)

School of Electronics and Information Engineering, Tianjin University, Tianjin 300072, *China*

(Received 18 May 2011; revised manuscript received 7 June 2011)

Density functional theory (DFT) calculations are employed to explore the NO_2-sensing mechanisms of pure and Ti-doped WO_3 (002) surfaces. When Ti is doped into the WO_3 surface, two substitution models are considered: substitution of Ti for W_{6c} and substitution of Ti for W_{5c}. The results reveal that substitution of Ti for 5-fold W forms a stable doping structure, and doping induces some new electronic states in the band gap, which may lead to changes in the surface properties. Four top adsorption models of NO_2 on pure and Ti-doped WO_3 (002) surfaces are investigated: adsorptions on 5-fold W (Ti), on 6-fold W, on bridging oxygen, and on plane oxygen. The most stable and likely NO_2 adsorption structures are both N-end oriented to the surface bridge oxygen O_{1c} site. By comparing the adsorption energy and the electronic population, it is found that Ti doping can enhance the adsorption of NO_2, which theoretically proves the experimental observation that Ti doping can greatly increase the WO_3 gas sensor sensitivity to NO_2 gas.

Keywords: adsorption, Ti doping, NO_2-sensing, density functional theory

PACS: 21.60.De, 21.60.Jz, 31.10.+z, 07.07.Df **DOI:** 10.1088/1674-1056/20/10/102101

1. Introduction

The detection of NO_2 is of importance for monitoring environmental pollution resulting from combustion processes, particularly industrial emissions or vehicle exhausts.[1−3] Semiconducting metal oxides such as WO_3, TiO_2, SnO_2, ZnO can be utilized as solid-state gas sensor materials and have been widely used for NO_2 detection,[2−4] by measuring the conductance changes in the surface phenomena in terms of gas adsorption and desorption.[5] WO_3 is an n-type semiconductor and shows good performance in NO_2-sensing, for instance, a high sensitivity, and a low-level concentration of NO_2 detection.[6] However, WO_3 gas sensors have a high operating temperature and slow response-recovery time.[7] So WO_3 is often modified with a small quantity of metal such as noble metals,[8] palladium (Pd), platinum (Pt), gold (Au), or transition metals, such as titanium (Ti)[9] to improve its NO_2-sensing properties. The sensing mechanism and the experimental phenomena have already been discussed, but there has been scant theoretical work. Therefore, it is necessary to understand the surface reactions at the solid–gas interface of pure WO_3 and doped WO_3 at the atomic level as a complement to experimental work, which would give great insight to the relevant experimental development.

In a previous work,[10] we discussed the surface energies of different WO_3 surfaces and learned that the (002) surface had minimum energy, in accordance with experiments in Refs. [7] and [11]. So, the WO_3 (002) surface was chosen as the best model to calculate NO_2 adsorption properties. It was found that gas adsorption can modify the band structure and order of electronic energy levels,[12,13] which may have a significant influence on determining the properties of the oxide as a gas sensor.

In this paper, experimentally, pure WO_3 and Ti-doped WO_3 thin films were prepared as gas sensors to detect NO_2; theoretically, based on density functional theory, the influence of Ti dopant on the surface properties of WO_3 (002) and benefits of the NO_2 adsorption, through comparing the interactions of NO_2 with pure and Ti-doped WO_3 (002) surfaces, were investi-

*Project supported by the National Natural Science Foundation of China (Grant Nos. 60771019 and 60801018), Tianjin Key Research Program of Application Foundation and Advanced Technology, China (Grant No. 11JCZDJC15300), Tianjin Natural Science Foundation, China (Grant No. 09JCYBJC01100), and the New Teacher Foundation of the Ministry of Education, China (Grant No. 200800561109).

†Corresponding author. E-mail: huming@tju.edu.cn

© 2011 Chinese Physical Society and IOP Publishing Ltd

gated. The main purpose of this paper is to clarify the effect of Ti doping on the sensitivity of the WO_3 (002) surface for the adsorption of NO_2 with respect to the pure surface.

2. Computational details and modeling system

2.1. Computational details

First-principles calculations based on density functional theory (DFT)[14,15] were performed using the commercial software CASTEP in Materials Studio (Version 5.0) of Accelrys Inc, which can provide accurate calculations of the energy and vibrational properties of the adsorption.[16,17] The widely used local density approximation (LDA) with the exchange correlation functional parameterized by Ceperley and Alder (CA-PZ) was adopted.[18] The real-space orbital cutoff was set to be 4.0 Å (1 Å = 0.1 nm), the force threshold for optimization was 0.01 eV and the Brilloiouin zone k-point sampling was performed in a $3 \times 4 \times 1$ Monkhorst–Pack scheme. The calculations were found to converge using an energy cut-off of 340 eV. The convergence criteria for structure optimization and energy calculation were set to be of medium quality with a tolerance for self-consistent field (SCF), energy, maximum force, and maximum displacement of 2.0×10^{-6} eV/atom, 2.0×10^{-5} eV/atom, 0.05 eV/Å, and 2.0×10^{-3} Å. A Fermi smearing of 0.1 eV was utilized. All the above parameters were kept fixed in all subsequent calculations. These values of the parameters correspond to a medium quality calculation which delivers the highest accuracy that is still computationally feasible for such large systems.

The surface calculations were performed using the slab method, in which three layers were used to approximate the surface. This was repeated in a periodic cell, with a vacuum gap used in the direction perpendicular to the surface. A gap of 15 Å was used in these calculations, which is expected to be sufficient to eliminate any interactions amongst mirror surfaces. The structural relaxations were done by means of a conjugate gradient minimization of the energy.

2.2. Modeling system

The crystal structures of WO_3 for gas sensors prepared under different conditions are not always exactly the same, which greatly influences their electronic structures and surface properties. The most stable surface of WO_3 is the (002) surface and is chosen as the adsorption surface. A supercell consisting of a (1×1) surface unit cell was used and a periodic slab model composed of three layers was adopted to simulate the WO_3 (002) surface as shown in Fig. 1. The outermost oxygen anions occupying bridging positions and coordinating cations W^{6+} are defined as O_{1c}, while in the second atomic layer, oxygen anions are in plane sites with 2-fold coordinates, marked as O_{2c}, cations W^{6+} in plane are 6-folds as W_{6c}, and unsaturated 5-fold W^{6+} as W_{5c} as well as fully coordinated with plane oxygen. The third atomic layer is constituted of sub-bridging oxygen atoms.

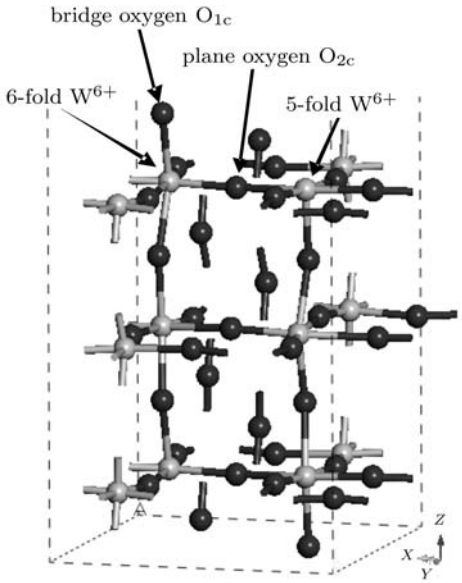


Fig. 1. Slab model of WO_3 (002) surface (light spheres represent W atoms; dark ones are O atoms).

First, NO_2 adsorption on the pure WO_3 (002) surface was studied. When the model of NO_2 adsorption on (002) surface was built, N atoms were chosen to connect to the surface, since it is easier for N to coordinate with O and W atoms.[19,20] In our work, there are four possible models. Figure 2(a) exhibits NO_2 adsorption on the O_{1c} site, named M_1; figure 2(b) shows the model of NO_2 adsorption on the O_{2c} site, marked M_2; figure 2(c) indicates the model of NO_2 adsorption on the W_{6c} site, named M_3, and figure 2(d) shows the model of NO_2 adsorption on W_{5c} site, denoted as M_4.

Next, we develop NO_2 adsorption on the Ti-doped WO_3 (002) surface. Based on the fact that the ionic radius of Ti^{4+} (0.605 Å) is as long as that of W^{6+} (0.6 Å),[21] it is most likely that the W^{6+} ions on the surface can be substituted by Ti^{4+} ions. Owing to the existence of two forms of W^{6+} ions, two substitution models were considered: substitution of Ti

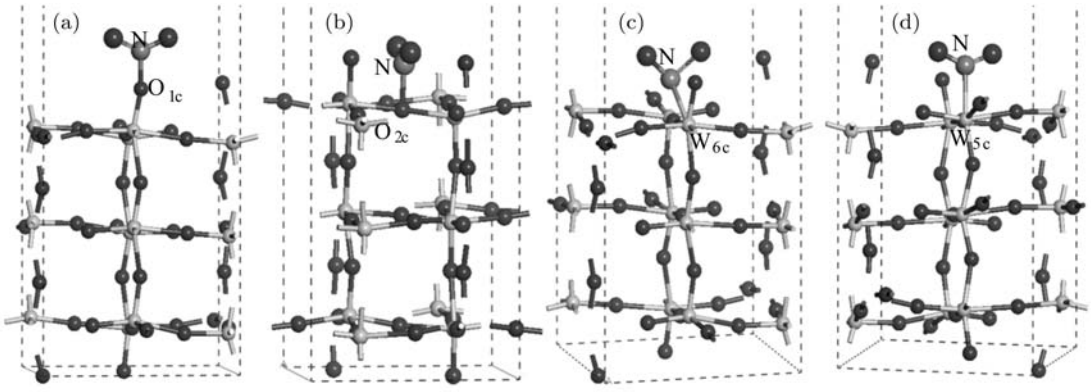


Fig. 2. NO_2 adsorption models on WO_3 (002) surface: (a) M_1 model; (b) M_2 model; (c) M_3 model; (d) M_4 model.

for W_{6c} and substitution of Ti for W_{5c}. Correspondingly, when NO_2 is adsorbed on the WO_3 (002) surface, there are still four models: NO_2 adsorption on bridging O_{1c} site (N_1), on plane O_{2c} site (N_2), on W_{6c} site (N_3), and doped Ti (N_4). The differences in adsorption energy and electronic population between the pure and the Ti-doped surfaces are discussed.

3. Computation results and discussion

3.1. Change of WO_3 (002) surface property

The calculated results of pure WO_3 (002) surface show that WO_3 is a direct band gap material with Fermi energy level sites in the band gap. Its surface energy is −38991.4916 eV, the band gap is 1.638 eV, and the Fermi energy is 3.69759 eV. The valence band mainly consists of the 2p, 2s states of O and 5d states of W, while the conduction band is dominated by W 2s states, and O 2p states.

3.1.1. Optimum Ti doping site of the WO_3 (002) surface

As mentioned above, W atoms have two forms, so there are two substitution models to be considered: substitution of Ti for W_{6c} and substitution of Ti for W_{5c}. The system energy of the two models were computed separately, and the result is that the energy of the former model (−38659.9883 eV) is higher than that of the latter (−38659.1011 eV). Based on equilibrium morphology theory, the crystal surface energy is related to its growing morphology and it prefers to crystallize toward a low-energy state;[22,23] the most stable doping structure of the Ti-doped WO_3 (002) surface is the substitution of a Ti atom for the 5-fold W atom and it is also the doped-model NO_2 adsorbing later.

3.1.2. Surface structure

Table 1 lists the changes of relative displacements of the WO_3 (002) surface outermost atoms compared with the Ti-doped WO_3 (002) surface structure optimized with the pure WO_3 (002) surface. It is found that Ti doping causes the surface structure of WO_3 (002) to change significantly. Apart from the one-fold O_{1c} moving inwards, the other atoms all drift outwards. For O_{1c} and W_{6c} atoms, the distance changes are both about 1 Å, with O_{1c} inside and W_{6c} outside. For the O_{2c} atom, the outside relaxation decreases from 1.8120 Å to 1.1017 Å. For the W_{5c} atom, it is substituted by Ti atom, and the displacement changes from 2.04638 Å out of the surface to 1.4741 Å into the surface. Because the surface configuration has changed significantly, we can expect that the Ti substitution for the W atom would have a great effect on the band structure and the density of states (DOS) of the surface.

Table 1. Relative displacements of outermost atoms after Ti doping.

Model	Relative displacement/Å			
	O_{1c}	O_{2c}	W_{6c}	W_{5c}/Ti
(002) surface	0.0175	–1.8120	–1.6073	–2.04638
Ti-doped (002) surface	1.0158	–1.1017	–0.6872	–1.4741

3.1.3. Electronic structure

Ti doping not only significantly affects the surface structure of WO_3 (002), but also causes the energy band structure to change substantially. The band gap of the WO_3 (002) surface after Ti doping decreases from 1.638 eV to 0.073 eV and the Fermi energy is −4.21821 eV. That is because the Ti atom causes a new orbit to appear in the middle of the band gap, called the hybrid orbital. We make a further analysis from the density of states (DOSs). The total DOSs of the pure and the Ti-doped WO_3 (002) surfaces are shown in Fig. 3(a). It can be seen that near the Fermi level the DOS is essentially unchanged, indicating that the contributions of Ti atoms and W atoms to the Fermi level are the same, but in a range from −39.9 eV to −27.6 eV, a new DOS line occurs compared with the Ti partial DOS (Fig. 3(b)). This line comes mainly from the Ti 2p orbital electron contribution. By comparison with the pure WO_3 (002) surface, the hybrid orbit and the additional states caused by Ti doping are the main reason for the change in the electronic structure of the WO_3 (002) surface.

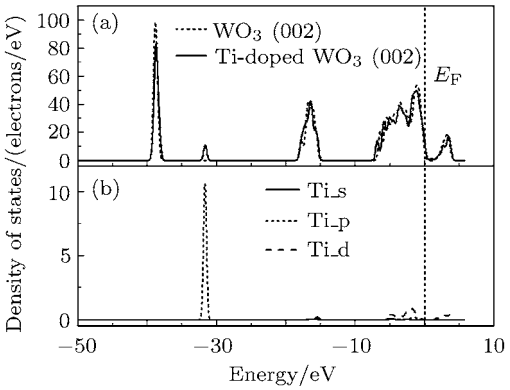


Fig. 3. DOSs and PDOSs of the Ti-doped WO_3 (002) surface: (a) DOSs of the pure and Ti-doped WO_3 (002) surfaces; (b) PDOSs of Ti.

3.2. Adsorption property of NO_2 on the pure WO_3 (002) surface

3.2.1. Adsorption energy

The system of NO_2 on pure WO_3 (002) was first optimized to calculate its physical properties. Then through the difference between the reconstructed surface of WO_3 (002) and the whole system, the adsorption energy and contribution from charge transfer were obtained. The adsorption energy can be defined as[24,25]

$$E_{\rm ads} = E_{\rm NO_2+Surf} - E_{\rm surf} - E_{\rm NO_2}, \qquad (1)$$

where $E_{\rm NO_2+surf}$ is the total energy for the slab with NO_2 adsorbed on the surface; $E_{\rm surf}$ and $E_{\rm NO_2}$ represent the total energies of surface and free NO_2 molecule, respectively.

Based on the theory of molecular orbits, the N atom is located at the centre of NO_2 molecule and its sp2 hybrid orbit and two O atoms form 2δ. In this study, the NO_2 molecule was located in a periodically repeated box of length 10 Å and energy −1138.883 eV. The adsorption energies of the four possible calculated models (M_1–M_4) for NO_2 adsorption on WO_3 (002) surface are represented in Table 2. It is obvious that all adsorption energies are negative, which means that NO_2 molecules were adsorbed in four sites spontaneously without any extra energy.[26] In terms of energy, NO_2 adsorption with the N-end oriented to the surface bridge oxygen (M_1 model) is the most stable and likely adsorption structure. This is also reasonable because O_{1c} has a free bond and is also the topmost atom. Thus, we now specifically discuss the adsorption properties of NO_2 on (002) surface O_{1c} adsorption.

Table 2. Adsorption energies of different models.

Calculated mode	WO_3 (002)	NO_2	M_1	M_2	M_3	M_4
Energy/eV	–38991.492	–1138.883	–40131.264	–40130.421	–40130.764	–40131.225
Adsorption energy/eV			–0.889	–0.046	–0.389	–0.850

3.2.2. DOS and electronic structure

Comparing the DOSs of the WO_3 (002) surface before and after NO_2 adsorption of model M_1 as shown in Fig. 4, it can be found that the adsorption has certain effects on the DOS of the whole surface. The most obvious is that all states shift toward the left after adsorption. The peak height in a range of -10 eV ~ 0 eV increases from 52 electrons/eV to 58 electrons/eV and the adsorption of NO_2 molecules inject three small electronic states into the band gap of the surface in a range of -25 eV ~ -10 eV. Therefore, the band gap of the WO_3 (002) surface after adsorption decreases by 1.475 eV from 1.638 eV to 0.163 eV and the most prominent effect of NO_2 adsorption is the shift of the Fermi level, by 1.42 eV towards the high-energy direction (−3.70 eV for WO_3 (002) surface and −2.28 eV

for the NO_2 adsorbed WO_3 (002) surface). Considering the distribution change of the electronic states of the surface, the raising of the Fermi level is the main reason for sensitive changes of the electrical properties of the surface.

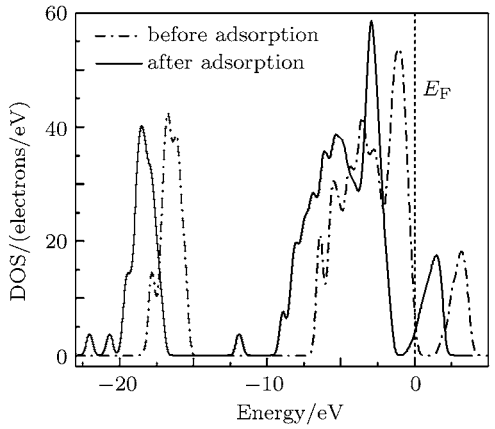


Fig. 4. DOSs of the WO_3 (002) surface before and after NO_2 adsorption.

3.2.3. Population analysis

Population analysis of the NO_2 molecule before and after adsorption is reported in Table 3. The results show that both N and O atoms have the same tendency: s orbital electron number is reduced and p orbital electron number is increased to some extent. However, the numbers are slightly different. The total electrons in the N atom decrease from 4.57 e to 4.39 e, while the increase in the O atoms is from 6.22 e to 6.60 e. The change of electron populations changes the bond length. From calculated results, it is known that the N–O bond length has a slight decrease in comparison with that of free NO_2, in which the N–O_1 bond length decreases from 1.22884 Å to 1.21833 Å and the N–O_2 bond length reduces from 1.23100 Å to 1.21819 Å. The free NO_2 molecules before adsorption are electrically neutral, while after adsorption, the N atom loses 0.18 e but the O atoms obtain 0.77 e, which means that the NO_2 molecule obtains 0.58 e. The obtained electrons are transferred from the WO_3 surface, which can increase the height of the barrier in the depletion region and reduce the conductance of the surface. Sensitivity varies with conductance, so WO_3 is widely used for NO_2 detection.

Table 3. Electron populations of NO_2 molecules before and after adsorption.

Atom	Before adsorption/e			After adsorption/e		
	s	p	Total	s	p	Total
N	1.37	3.2	4.57	1.19	3.20	4.39
O_1	1.85	4.37	6.22	1.83	4.77	6.60
O_2	1.85	4.37	6.22	1.83	4.77	6.60

3.3. Adsorption properties of NO_2 on the Ti-doped WO_3 (002) surface

3.3.1. Adsorption energy

The calculated results of adsorption energies for NO_2 on the Ti-doped WO_3 (002) surface are summarized in Table 4. It is found that the most favourable adsorption geometry of NO_2 on the Ti-doped surface is the NO_2 adsorbed on the bridge oxygen atom (model N_1) with an adsorption energy of 3.384 eV, which is much larger than the value 0.889 eV calculated for the pure surface. Ti doping did not change the optimum NO_2 adsorption site of the surface, which is the bridge oxygen site O_{1c} owning a free bond. So defect sites are the ones on which NO_2 is more easily adsorbed.

Table 4. Adsorption energies of different models.

Calculated mode	Ti-WO_3 (002)	NO_2	N_1	N_2	N_3	N_4
Energy/eV	–38659.988	–1138.616	–39801.000	–39800.766	–39800.762	–39799.672
Adsorption energy/eV			–3.384	–2.162	–2.158	–1.068

Moreover, energies released by NO_2 adsorption on the Ti-doped WO_3 (002) surface (model N_1–N_4) are all larger than those by NO_2 adsorption on the pure WO_3 (002) surface (model M_1–M_4). From the definition of adsorption energy in Eq. (1), large adsorption energy means the energy of the whole system has greater reduction after adsorption; therefore, the possibility of NO_2 self-adsorption on WO_3 is increased. The results indicate that doped Ti has a significant influence on the adsorption energies of the models to some extent. It can be seen that doped Ti can reduce surface energy, making the NO_2 adsorption easier and improving the sensor activity.

3.3.2. Population analysis

The electron population of the NO_2 molecule adsorbed on the Ti-doped WO_3 surface was calculated, and the results are listed in Table 5.

Table 5. Electron populations of the NO_2 molecule before and after adsorption.

Atom	Before adsorption/e			After adsorption/e		
	s	p	Total	s	p	Total
N	1.37	3.20	4.57	1.20	3.21	4.41
O_1	1.85	4.37	6.22	1.82	4.78	6.61
O_2	1.85	4.37	6.22	1.82	4.78	6.61

Similarly, the results show that N atom loses 0.16 e (from 4.57 e to 4.41 e) but two O atoms obtain 0.78 e in total (where the electron number on each O atom increases from 6.22 to 6.61, i.e., each atom increases by 0.39 electrons on average), which means that the NO_2 molecule obtains 0.62 e from the surface of Ti-doped WO_3 (002), and the electron number is larger than the value 0.58 e transferred on the pure surface. The larger calculated results of the electron population prove that Ti-doping can greatly increase WO_3 sensor sensitivity to NO_2 gas. This is consistent with the experimental results given below.

4. Experimental

4.1. Fabrication of the sensing elements

The sensing elements were fabricated as follows. First, interdigital Pt electrodes were deposited on clean Al_2O_3 ceramic substrates (0.9 cm × 2.4 cm) by RF magnetron sputtering. Then, WO_3 nano-thin film was deposited on the top surface of the Pt film. TiO_2 thin film as a modified layer was then sputtered on the uppermost. In all sputtering work we used a DPS-III ultra-high vacuum facing target magnetron sputtering system from the Chinese Academy of Sciences in Shenyang Scientific Instrument Development Center Co., Ltd. The specific sputtering conditions of Pt, WO_3, and TiO_2 thin films are shown in Table 6. Finally, the elements were all annealed in a high-temperature heating furnace at 450 °C in dry air for 4 h. The structure of the sensor is given in Fig. 5. The sensors were loaded into a homemade static gas test system and connected to external electronics to monitor their resistance change independently.[27] The sensitivity is defined as

$$S = (R_{\text{gas}} - R_{\text{air}})/R_{\text{air}}, \tag{2}$$

where R_{air} is the resistance in ambient air and R_{gas} is the maximum resistance in NO_2 and air-mixed gas.

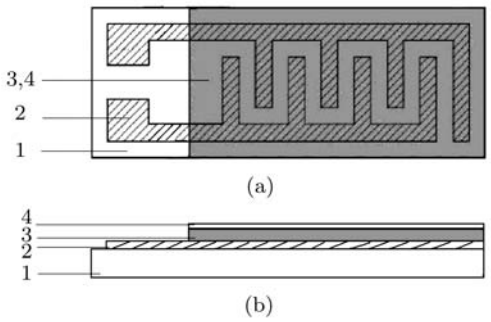


Fig. 5. Schematic diagram of TiO_2–WO_3 thin film gas sensor (a): top view, (b): side view, 1: Al_2O_3 substrate, 2: Pt interdigital electrode, 3: WO_3, 4: TiO_2 thin film).

Table 6. Preparation conditions of Pt, WO_3, and TiO_2 thin films in TiO_2–WO_3 gas sensor, RT: room temperature.

Film	Sputtering targets	Sputtering gas	Working pressure/Pa	Sputtering power/W	Substrate temperature	Thickness/nm
Pt	99.95%Pt	Ar	2.0	70	RT	90
WO_3	99.99%W	60%Ar:40%O_2	1.0	80	RT	150
TiO_2	99.99%Ti	90%Ar:10%O_2	2.0	100	RT	40

4.2. Sensing characteristics of elements and discussion

As described in Ref. [28], sputtering a certain thickness of TiO_2 film on WO_3 film and substituting Ti^{4+} for W^{6+} partly in the processing of annealing can realize the effects of Ti doping. Figure 6 shows the relationships between sensitivity and NO_2 gas concentration of pure WO_3 and TiO_2–WO_3 thin films at an operating temperature of 120 °C. It can be seen clearly that the TiO_2–WO_3 film has a much higher sensitivity to various concentrations of NO_2 gas than the pure WO_3 film at the optimum operating temperature. This phenomenon can be explained by the theoretical results derived above. As an n-type semiconductor, the carriers of WO_3 are mainly electrons.

When oxidizing gas NO_2 was injected into the test chamber, the resistance of the sensor became large and the number of electrons diminished. In the previous calculation, on the one hand, for the Ti-doped WO_3 model, hybrid orbitals appeared in the middle of the band gap due to Ti doping and they can generate additional energy levels as an additional acceptor level, which hinders the valence band electrons from transiting into the conduction band directly. So it is more difficult to transit electrons. On the other hand, NO_2 molecules obtain more electrons from the surface of Ti-doped WO_3 than from the surface of the pure WO_3, which means Ti-doped WO_3 had fewer carriers than the pure WO_3 after NO_2 adsorption. As a result, its resistance increased more rapidly, and sensitivity was higher.

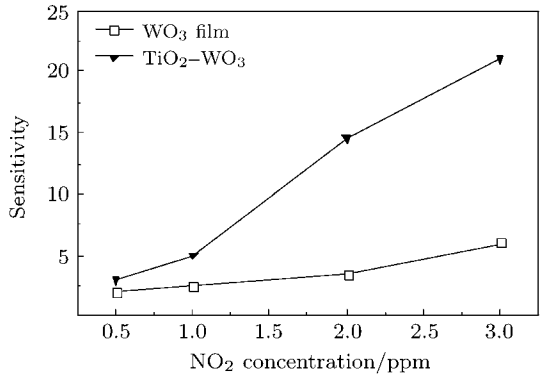


Fig. 6. Relationships between sensitivity and NO_2 gas concentration of pure WO_3 and TiO_2–WO_3 thin films at an operating temperature of 120 °C.

5. Conclusion

In this paper, first-principles calculations based on DFT are used to investigate the change of WO_3 (002) surface properties caused by Ti dopant. Two substitution models are considered: substitution of Ti for W_{6c} and substitution of Ti for W_{5c}. The energy calculation indicates that the most stable doping structure of Ti-doped WO_3 (002) surface is the substitution of a Ti atom for the 5-fold W atom. Ti doping greatly affects both the surface structure and the energy band structure of WO_3 (002). The band gap of WO_3 (002) surface, after doping with Ti, decreases from 1.638 eV to 0.073 eV. The decreased band gap and the additional states caused by Ti doping are the main reason for the change in the electronic structure of the WO_3 (002) surface.

The properties of NO_2 adsorption on pure and Ti-doped WO_3 (002) surfaces are studied through four separate adsorption models. It is found that all the adsorption energies are negative and NO_2 molecules are adsorbed on the surface spontaneously. In terms of energy, the most stable and likely NO_2 adsorption structures are both N-end oriented to the surface bridge oxygen O_{1c} site (Model M_1 and N_1). O_{1c} has a free bond and is a defect site. So, defect sites are the ones on which NO_2 is adsorbed more easily. The adsorption energy (3.384 eV) for NO_2 on the Ti-doped WO_3 (002) surface is much larger than the value (0.889 eV) calculated for the pure surface. The results indicate that doped Ti can reduce surface energy and make NO_2 adsorption easier. This is helpful for increasing the sensitivity to NO_2. The electron population of NO_2 molecules adsorbed on the Ti-doped WO_3 surface provides another explanation: considering the value 0.58 e of electron transfer from the pure surface, the Ti-doped surface obtains more electrons after NO_2 adsorption. The results theoretically prove the fact that Ti doping can improve the sensitivity of NO_2 on the WO_3 surface for gas sensors.

Based on the above analyses, we know that when the gas molecule is adsorbed on the surface, the electronic conductance of the gas sensor changes. These results are shown to be in good accord with our experimental results and conducive to the understanding of the sensing mechanism of WO_3-based gas sensors.

References

[1] Ma H L, Fan D W and Niu X S 2010 *Chin. Phys.* B **19** 076102

[2] Teoh L G, Hon Y M, Shieh J, Lai W H and Hon M H 2003 *Sensors and Actuators* B **96** 219

[3] Hua Z Q, Wang Y, Wang H Q and Dong L 2010 *Sensors and Actuators* B **150** 588

[4] Yang Y R, Yan X H, Guo Z H and Deng Y X 2008 *Chin. Phys.* B **17** 3433

[5] Jo S E, Kang B G, Heo S, Song S and Kim Y J 2009 *Current Appl. Phys.* **9** e235

[6] Ghimbeu C M, Lumbreras M, Siadat M and Schoonman J 2010 *Mater. Sci. Semicond. Proce.* **13** 1

[7] Qin Y X, Hu M and Zhang J 2010 *Sensors and Actuators* B **150** 339

[8] Penza M, Martucci C and Cassano G 1998 *Sensors and Actuators* B **50** 52

[9] Chaudhari G N, Bende A M, Bodade A B, Patil S S and Sapkal V S 2006 *Sensors and Actuators* B **115** 297

[10] Hu M, Zhang J, Wang W D and Qin Y X 2011 *Chin. Phys.* B **20** 082101

[11] Guo Y F, Quan X, Lu N, Zhao H M and Chen S 2007 *Environ. Sci. Technol.* **41** 4422

[12] Wang C, Wang F F, Fu X Q, Zhang E D and Xu Z 2011 *Chin. Phys.* B **20** 050701

[13] Le L C, Ma X G, Tang H, Wang Y, Li X and Jiang J J 2009 *Acta Phys. Sin.* **59** 1314 (in Chinese)
[14] Kresse G and Furthmuller J 1996 *Phys. Rev.* B **54** 11169
[15] Hohenberg P and Kohn W 1964 *J. Phys. Rev.* **136** B864
[16] Prades J D, Cirera A, Morante J R, Pruneda J M and Ordejon P 2007 *Sensors and Actuators* B 2007 **126** 62
[17] Neyman K M and Illas F 2005 *Catalysis Today* **105** 2
[18] Kotochigova S, Levine Z H, Shirley E L, Stiles M D and Clark C W 1997 *Phys. Rev.* A **55** 191
[19] Ma S Y and Wang S Q 2008 *Chin. Phys.* B **17** 3856
[20] Ying M J, Zhang P and Du X L 2009 *Chin. Phys.* B **18** 275
[21] Imawan C, Solzbacher F, Steffes H and Obermeier E 2000 *Sensors and Actuators* B **64** 193
[22] Xu X L, Chen Z H, Li Y, Chen W K and Li J Q 2009 *Surf. Sci.* **603** 653
[23] Bentmann H, Demkov A A, Gregory R and Zollner S 2008 *Phys. Rev.* B **78** 205302-1
[24] Xue Y B, Tang Z A and Wei G F 2007 *Chinese Journal of Sensors and Actuators* **20** 2364 (in Chinese)
[25] Yang Y 2009 *Chin. Phys.* B **18** 603
[26] Xue Y B and Tang Z A 2009 *Sensors and Actuators* B **138** 108
[27] Sun F Y, Hu M, Sun P, Zhang J and Liu B 2010 *J. Nanosci. Nanotechnol.* **10** 7739
[28] Yin Y Z, Hu M, Feng Y C, Chen P and Liu Z G 2008 *Piezoelectrics & Acoustooptics* **30** 588 (in Chinese)